Supporting Information

Ultrathin silica integration for enhancing reliability of microfluidic photoionization detectors

Xiaheng Huang[1,2,3,4,†], Ruchi Sharma[1,3,4,†], Anjali Devi Sivakumar[1,2,3,4], Shuo Yang[1,3,4], and Xudong Fan[1,3,4,*]

[1]Department of Biomedical Engineering,
University of Michigan, Ann Arbor, MI 48109, USA

[2]Department of Electrical Engineering and Computer Science,
University of Michigan, Ann Arbor, MI 48109, USA

[3]Center for Wireless Integrated MicroSensing and Systems (WIMS[2]),
University of Michigan, Ann Arbor, MI 48109, USA

[4]Max Harry Weil Institute for Critical Care Research and Innovation
University of Michigan, Ann Arbor, MI 48109, USA

†: Equal contribution

*: Corresponding author: xsfan@umich.edu

Table of Contents

Materials and Methods

Materials

Analytical standard grade VOC analytes (see Table S1 for details) were purchased from Sigma Aldrich (St. Louis, MO). P-type/Boron Prime silicon (Si) wafers (100 mm in diameter, 400 μm thick, 0.001-0.005 Ω-cm, double-sided-polished (DSP)) were from Ultrasil. Borofloat 33 Pyrex glass wafers (P/N 517) were from University Wafer. Single crystal MgF_2 and LiF substrates (<100> orientation, 10 x 10 x 0.5 mm in dimension, DSP, Ra (surface roughness) < 1.5 nm) were from BIOTAIN CRYSTAL CO., LIMITED. Kr VUV lamp (P/N 043-257) was from MOCON (part of AMETEK). Ar VUV lamp (P/N 050-0001-000 (RAE)) was from EQUIPCO. UV-curable epoxy (P/N NOA 68T) was from Norland Products. The transformer (P/N ZS1052(H)-ND) for Kr lamp excitation was from Digikey. The transformer (10KV High Frequency High Voltage Transformer Booster Coil Inverter) for Ar lamp excitation was from eBay. All materials were used as purchased without further purification or modification.

μPID packaging

The integrated microfluidic chip was electrically packaged on a printed circuit board by wire bonding the two gold electrode contacts with aluminum wires of 50 μm diameter using a wedge bonder. Then, two 10 cm long guard columns were inserted into the inlet and outlet ports, respectively, and hermetically sealed with UV-curable epoxy. Finally, the Kr (or Ar) lamps with built-in MgF_2 (or LiF) windows were mounted on top of the integrated MgF_2 (or LiF) interlayer window and sealed with UV-curable epoxy. Adhesive copper tapes were then applied to the VUV lamps to form two excitation electrodes facing each other for plasma generation. An in-house developed circuit was used for plasma generation and readout.

μPID sensitivity and reliability characterization

The sensitivity of the μPIDs was evaluated using an Agilent 6890 benchtop gas chromatography (GC) equipped with a thermal injector and a flame ionization detector (FID). 99.999% Helium was used as the carrier gas with a flow rate of 3 mL/min. All measurements were done at room temperature with only guard columns for fluidic connections. For reliability measurement, the μPID was fluidically connected to the FID in series, which served as the calibration detector assuming no degradation. The analytes were injected through the thermal injector (250 ºC) with a reference FID signal in the range of 200 pA to 500 pA to ensure similar and consistent injections for each measurement. The relative sensitivity of a μPID under test is

defined as the ratio of peak areas of μPID over FID. The time evolution of the relative sensitivity over certain aging conditions (*e.g.*, moisture or plasma exposure) was recorded in reliability tests.

Aging condition for moisture reliability test

Between relative sensitivity measurements, the μPIDs were aged with plasma turning off and without carrier gas flow in the lab ambient with a temperature of 19.7±0.7 ºC and a relative humidity of 41.5±10.4 % recorded by a thermometer *in-situ*.

Argon plasma chamber setup for Ar plasma exposure reliability test

An Ar plasma chamber (Harrick Plasma PDC-32G) was used to simulate LiF substrate degradation when exposed to plasma inside an Ar lamp. The RF plasma chamber was first pumped down to a low pressure below the atmosphere. 99.999% Ar gas was then fed into the chamber in a constant flow = 150 mL/min before the RF power was turned. The LiF substrates were placed at the same location inside the chamber during each aging cycle.

UV-VIS transmission characterization

The transmission spectra of the MgF_2 and LiF substrates were taken a Woollam M-2000 ellipsometer from 190 nm to 900 nm.

Atomic force microscopy (AFM) characterization

Surface roughness of the MgF_2 substrates before and after silica coating was characterized using a Bruker ICON AFM with tapping mode in the air. The scan area was 5 μm x 5 μm. Multiple positions on each sample were scanned for consistency.

Crystalline structure characterization by X-ray diffraction (XRD)

The crystalline structure of LiF and MgF_2 was determined by XRD technique. The samples were measured in reflection mode on a Rigaku Ultima 4 system. A parallel beam of Cu K-alpha excitation obtained from Rigaku's patented CBO (Cross-Beam-Optics) device was used as an X-ray source. X-ray tube runs at 40 kV and 44 mA. Cu K-beta was filtered by a 20-micron Ni foil.

LiF transmission restoration by thermal bleaching and DUV bleaching

Degraded LiF windows were thermally bleached by thermal annealing the sample on a hot plate at 350 ºC in ambient. Note that since the LiF window is susceptible to thermal shock, the LiF samples were first placed on the hotplate at room temperature before ramping to high temperatures. The Deep UV (DUV) bleaching was achieved by placing the sample under the illumination of 2400 μW/cm^2 at 245 nm (UVP UVG-11 P/N 95-0016-14) in ambient. The UV lamp's illumination power was calibrated using a UV meter. The DUV illumination also generated additional heat that raised the temperature of the sample in contact with the UV lamp surface to ~50 ºC.

Chemical composition characterization by X-ray photoelectron spectroscopy (XPS)

XPS spectra of fresh and aged LiF were collected using a Kratos Axis Ultra XPS with a monochromated Al Kα X-ray source (10 mA, 12 kV). The spot size was 700 μm × 300 μm. An Argon ion sputtering source with a sputtering rate of 0.025 nm/s was used for depth profiling. The sputtering duration was 1000 s (corresponding to 25 nm) for each depth step. Survey scans were used to quantify the atomic compositions at each depth. Core scans of Li 1 s level were used to investigate the binding environment of Li at each depth. The binding energies were calibrated to that of adventitious surface carbon (284.8 eV). The fresh LiF was measured right after being unpacked from a vacuum bag. The LiF were aged in the lab ambient (*i.e.*, temperature = 19.7±0.7 ºC and relative humidity = 41.5±10.4 %) for 1000 hours before measurement.

Analyte	Ionization potential (eV)
Xylene	8.56
Toluene	8.82
Benzene	9.25
Octane (C_8)	9.82
Heptane (C_7)	10.08
Hexane (C_6)	10.18
Ethanol	10.47
Methanol*	10.85
Formaldehyde*	10.86
Dichloromethane*	11.33
Chloroform*	11.37
Carbon Tetrachloride*	11.47

Table S1. Tested analytes with respective ionization potentials. "*" marks the analytes with IP >10.6 eV, which can only be detected by an Argon PID.

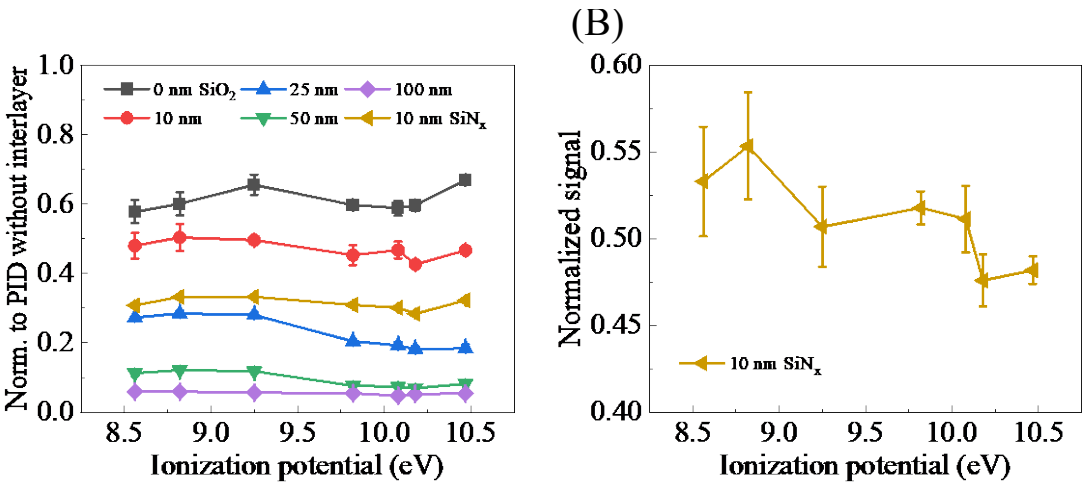

Figure S1. (A) Normalized signal of DUT with silica thickness = 0, 10, 25, 50, and 100 nm; and with 10 nm SiN_x. The normalization is defined as the ratio of peak areas of respective analytes (with corresponding ionization potentials) between the DUT and the calibration PID. (B) Normalized signal for 10 nm SiN_x vs. ionization potential. The normalization is defined as the ratio of peak areas of respective analytes (with corresponding ionization potentials) between the DUT with a 10 nm SiN_x coating and the DUT having a bare interlayer without any coating. Error bars were obtained with 3 measurements.

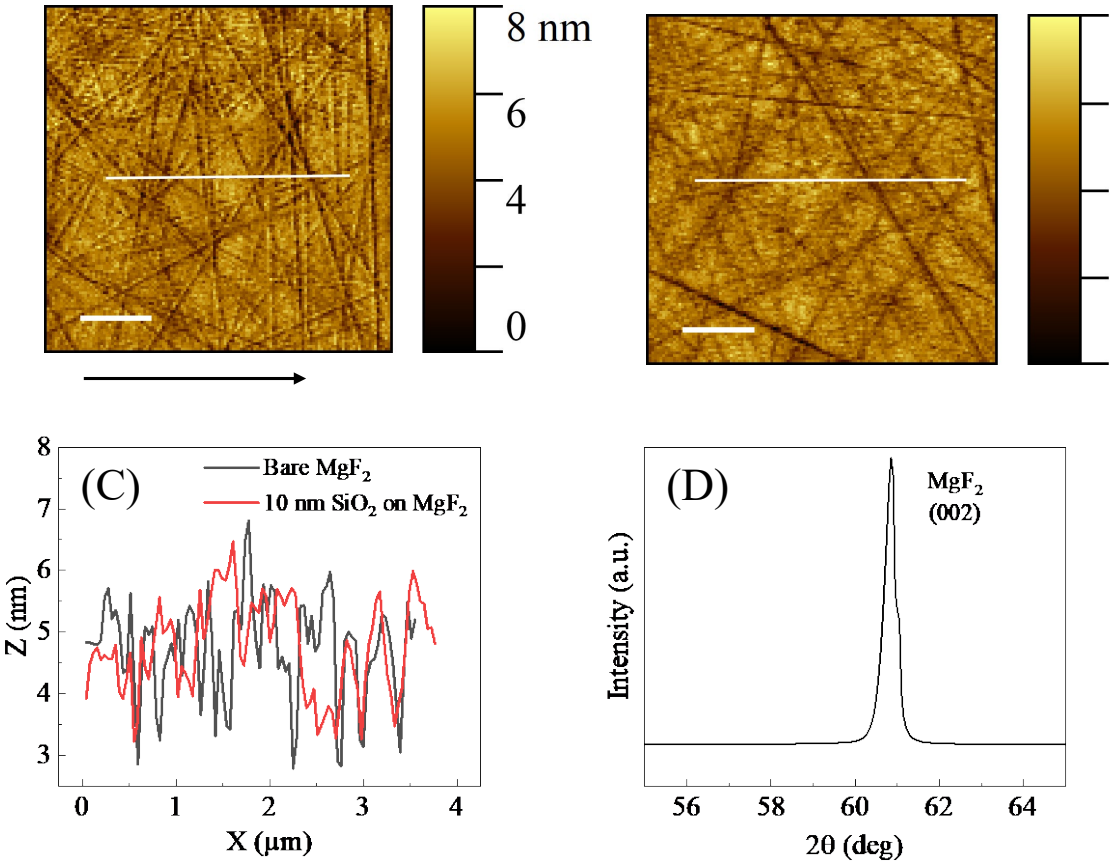

Figure S2. AFM images of (A) bare MgF_2 and (B) 10 nm silica on MgF_2. (C) One-dimensional cross-section comparison from the white intersection lines in (A) and (B). (D) X-ray diffraction of the MgF_2 substrate, indicating the single-crystal nature of MgF_2. The random line features in (A) and (B) were generated by the polishing process of the MgF_2 surface.

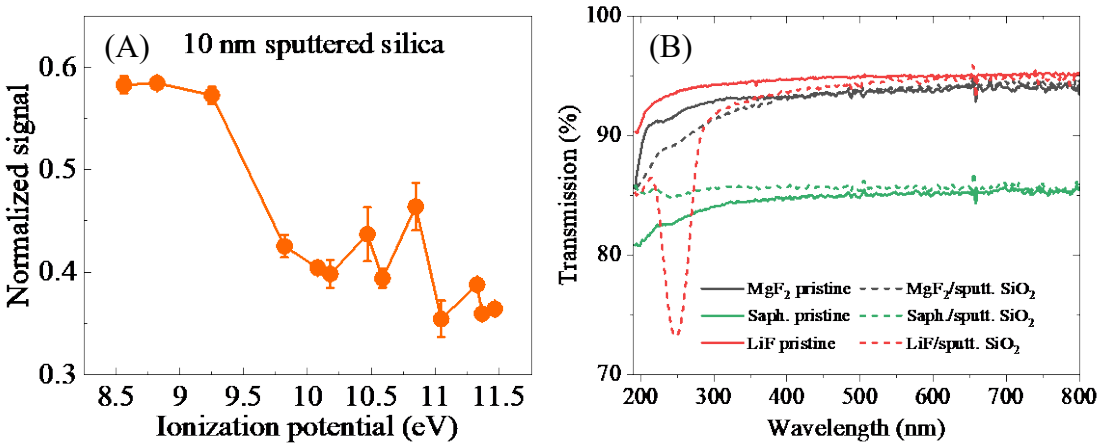

Figure S3. (A) Normalized signal for 10 nm sputtered silica vs. ionization potential. The normalization is defined as the ratio of peak areas of respective analytes (with corresponding ionization potentials) between the DUT with a 10 nm silica coating and the DUT having a bare LiF interlayer without any coating. The tested analytes are listed in Table S1. (B) Transmission spectra of pristine and silica-sputtered MgF_2, sapphire, and LiF substrates. LiF substrate developed a color center (at wavelength = 250 nm) due to exposure to Ar plasma during the sputtering process.

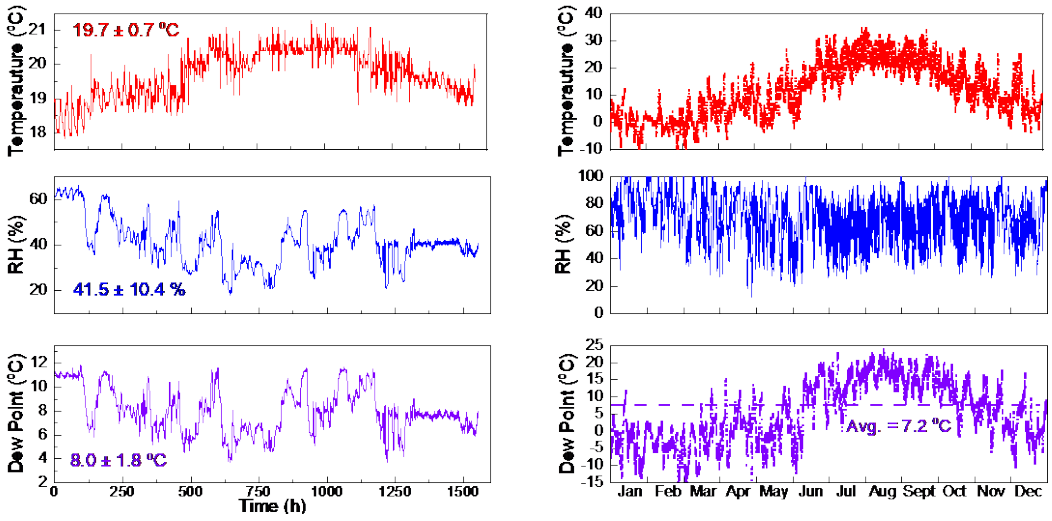

Figure S4. Temperature, relative humidity, and dew points of (A) the ambient condition during aging periods of PIDs in Figure 3(B). (B) Local climatological data in 2020 at Michigan, Detroit Metro Airport station (National Centers for Environmental Information).

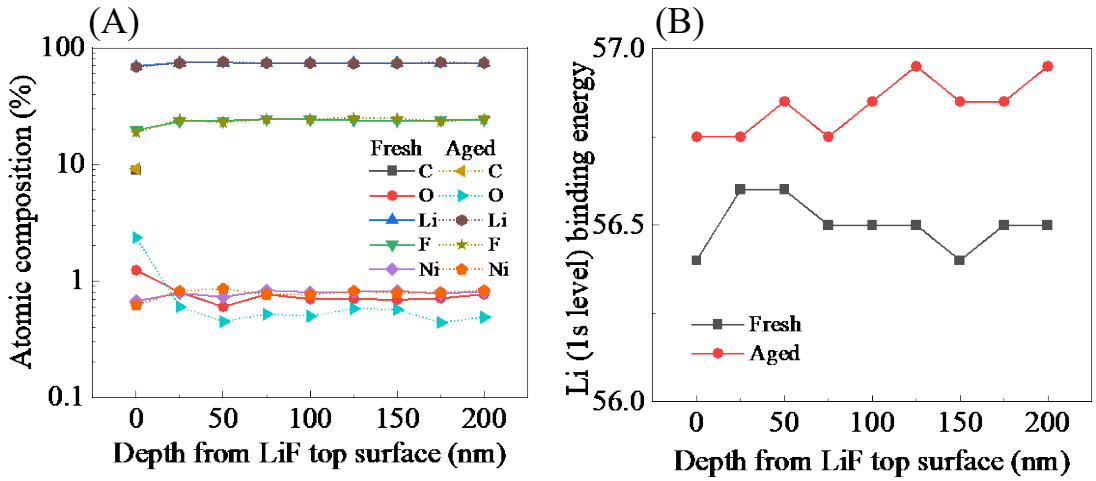

Figure S5. (A) Atomic compositions and (B) binding energy of Li 1 s level of the fresh and aged LiF vs. depth from LiF top surface. The atomic compositions were extracted from the survey scans at each depth. Each depth step is 25 nm. Note that the element carbon only appeared on the surface (*i.e.*, depth = 0 nm) of LiF. The binding energies were extracted by the core scans of Li 1 s level at each depth. The aged LiF were aged in the lab ambient (i.e., temperature = 19.7±0.7 ºC and relative humidity = 41.5±10.4 %) for 1000 hours before measurement.

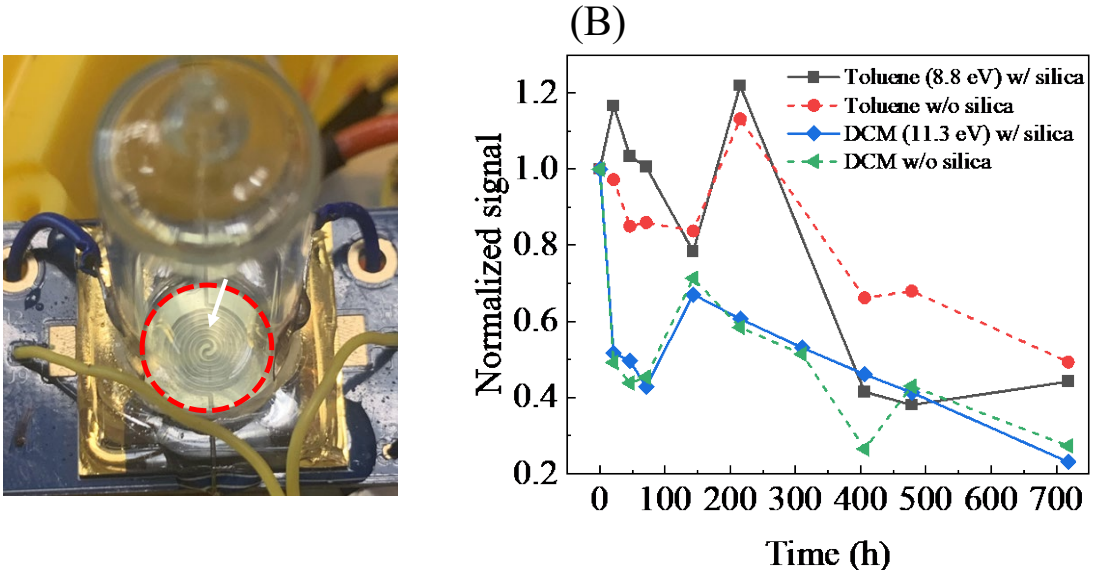

Figure S6. (A) Photo of an aged Ar-SIPID assembly. The dashed circle indicates the yellowish aged built-in LiF window. (B) Normalized signal of Ar-SIPIDs (with and without silica) for toluene (IP = 8.8 eV) and dichloromethane (DCM, IP = 11.3 eV) vs. aging time.

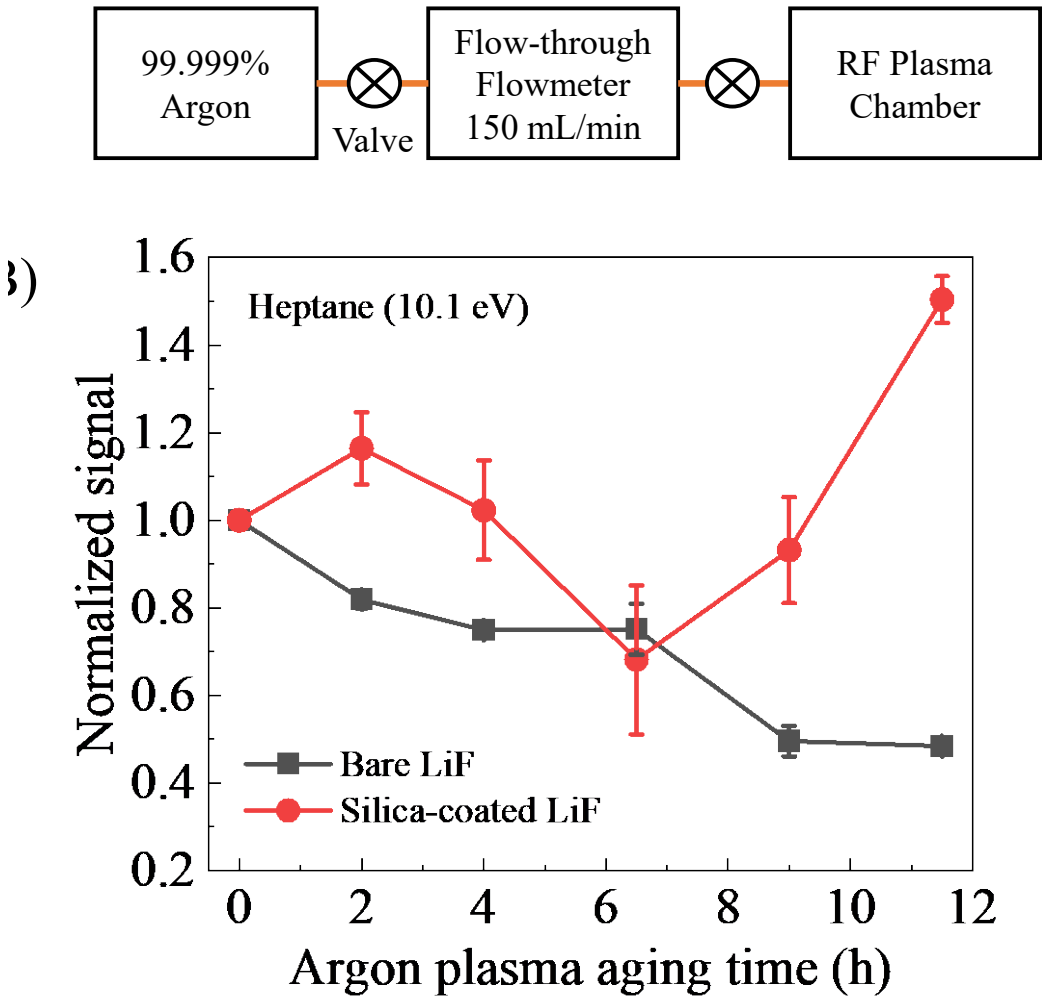

Figure S7. (A) Setup of Ar plasma chamber for simulating the aging from an actual Ar lamp. The RF plasma chamber was first pumped down to a pressure below the atmosphere. 99.999% Ar gas is then fed into the chamber for generating Argon plasma. Two valves and a flow-through flowmeter are used for controlling and monitoring the Argon flow. (B) Normalized signal of the device in Figure 5(B) with respect to the argon plasma aging time for both bare and silica-coated LiF interlayer (10 nm coated on both sides) using heptane (IP = 10.1 eV) as the analyte. The signal is normalized to that obtained at the 0^{th} hour for each interlayer.

Restoration of aged LiF windows by thermal and DUV bleaching

We demonstrate solutions to restore the degraded VUV transmission and color centers. The unaltered single-crystal morphology of the degraded built-in LiF (see Figure S8) suggests that the observed color centers could be attributed as a recoverable crystallographic defect in which an anionic vacancy is occupied by one or more unpaired electrons that can therefore absorb light and generate color centers. It is known that such color centers developed in alkali halide crystals can be bleached by thermal annealing or DUV illumination[1-3]. We therefore apply these two methods to restore two pairs of aged built-in LiF windows and their corresponding aged LiF interlayers in Figure 4(A).

Figure S9(A) shows the thermal bleaching results. In the severely aged built-in LiF window, the F center was eliminated after 68 hours of bleaching, while the M center disappeared much faster in only 3 hours. The interlayer LiF also had a fast recovery (3 hours) of its much less degraded F center. The F band recovery rates can be inferred from Figure S9(C). Both F bands in either built-in or interlayer LiF were recovered by thermal bleaching. As a result, the yellowish aged LiF window became clear again (see the pictures in the inset of Figure S9(A)). Compared to the complete elimination of color centers by thermal bleaching, DUV bleaching can only partially reduce the F center and M center of the degraded built-in LiF window at a slower rate as shown in Figures S9(B) and (C). In fact, the F center was blue-shifted as it recovered, which might indicate formation of new color centers caused by the DUV itself. Nevertheless, the F center in the aged interlayer LiF was restored entirely by DUV bleaching.

More importantly, we next qualitatively examined whether such bleaching could restore the transmission in the VUV range concomitantly with the UV-VIS range by using the device structure in Figure S10(A), which is similar to Figure 5(B). “Built-in LiF” referred to the similarly aged LiF window removed from an Ar lamp that was exposed to Ar plasma and visually discolored. By thermal bleaching (Figure S10(B)), the VUV transmission of an aged built-in LiF window enhanced progressively ~5 times at IP = 10.1 eV accompanied with its F center recovered from 60% to 80% (Figure 10(B) inset). In contrast, DUV bleaching was not as effective for recovering VUV transmission, despite significant restoration was seen in the UV-VIS range (Figure S10(C)). Therefore, thermal bleaching is considered an effective bleaching method throughout VUV to UV-VIS range, while DUV bleaching only cures the color centers in the UV-VIS range. Lastly, we explored the possibility to thermally recover an aged Ar lamp *in situ* by placing its intact built-in LiF window directly on the surface of a 350 ^{o}C hotplate in ambient. However, we found that the bonding between the lamp glass body and

the built-in LiF window failed after just 20 minutes of annealing (see Figure S11), which led to Ar gas leakage from inside and rendered the lamp useless. It is learned that a new bonding method that can withstand high temperatures (not necessarily 350 ºC) is needed to practically implement such VUV window restoration methods.

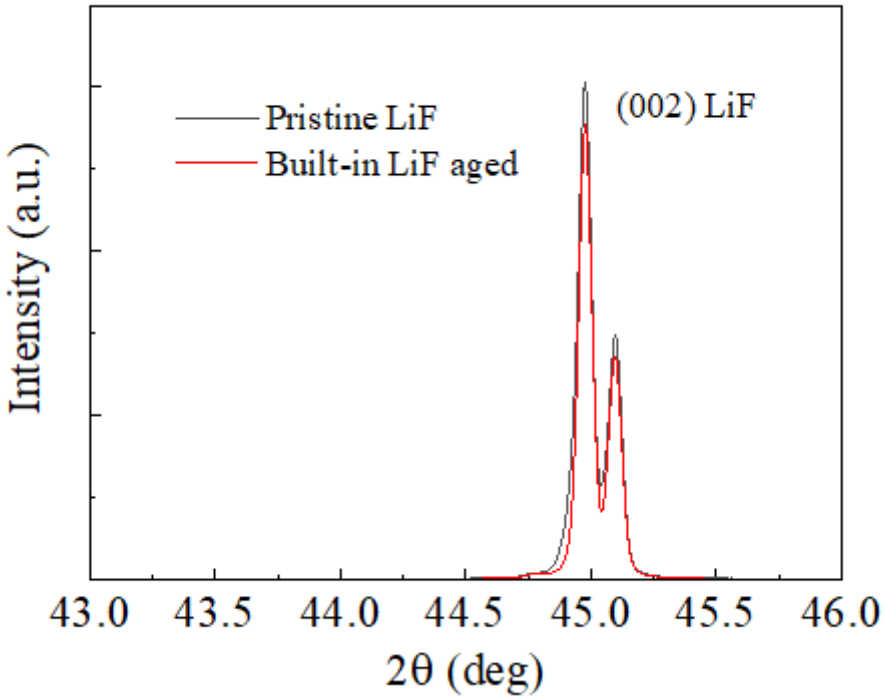

Figure S8. X-ray diffraction (XRD) patterns of a pristine LiF and the aged built-in LiF window as shown in Figure 3. The result suggests that the single-crystalline structure of the LiF remained unchanged after being exposed to Argon plasma.

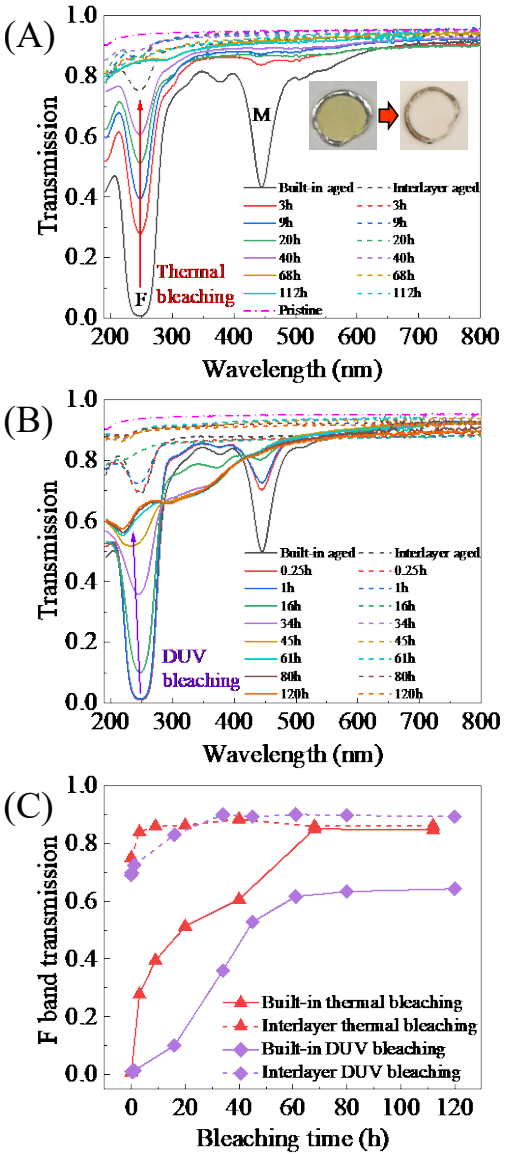

Figure S9. Transmission spectra of aged built-in and interlayer LiF using (A) thermal bleaching (annealing at 350 ºC in ambient) and (B) deep ultraviolet (DUV) bleaching (illuminated under 2400 μW/cm2 at 245 nm in ambient). All aged LiF samples were dissembled from the Ar-SIPID after 700 h of aging shown in Figure 4(B). F and M refer to the F color center and the M color center, respectively. Inset in (A) shows the photos of the built-in LiF sample at the 0th h and after 40 h of thermal bleaching. (C) F band (250 nm) transmission vs. bleaching time of aged built-in and interlayer LiF samples extracted from (A) and (B), respectively. The arrows in (A) and (B) indicate the F band trend during thermal and DUV bleaching processes.

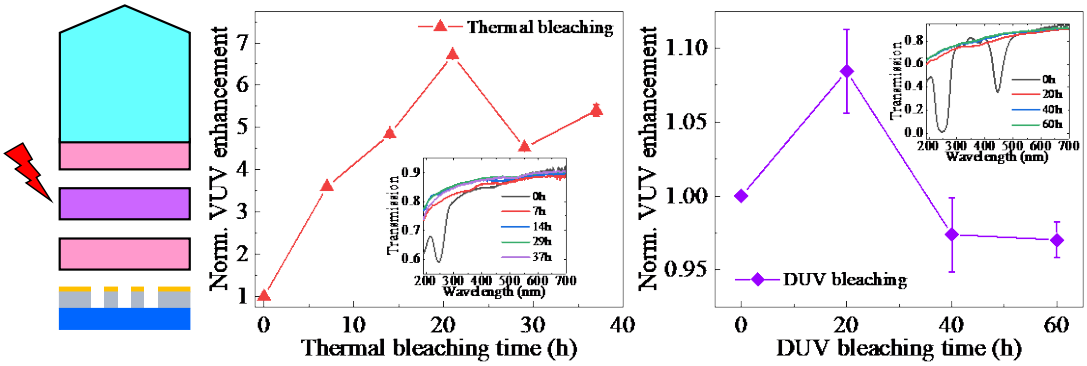

Figure S10. (A) Device structure for testing the VUV transmission enhancement of an aged built-in LiF interlayer by thermal bleaching. The aged built-in LiF was dissembled from an aged Ar-lamp and bleached by thermal annealing or DUV illumination. (B) VUV transmission enhancement vs. thermal bleaching time. Heptane (IP = 10.1 eV) was used as the test analyte. Inset: corresponding UV-VIS transmission spectra of the tested built-in LiF at different thermal bleaching times. (C) VUV transmission enhancement vs. DUV bleaching time. Benzene (IP = 9.2 eV) was used as the test analyte. Inset: corresponding UV-VIS transmission spectra of the tested built-in LiF at different DUV bleaching times. The VUV enhancement is normalized to the relative sensitivity obtained at the 0th hour. Error bars were obtained with 3 measurements.

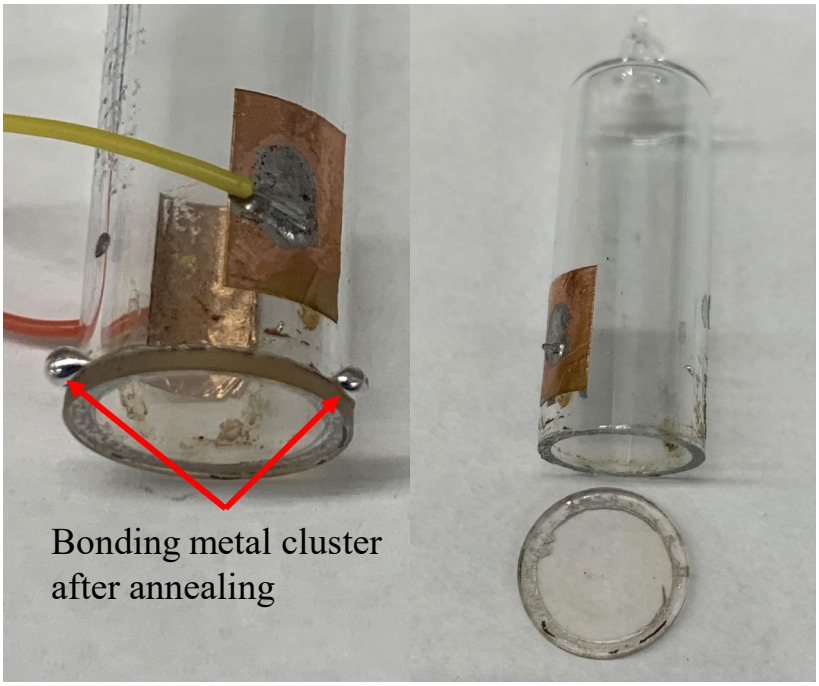

Figure S11. Photographs of an aged Ar lamp thermally annealed at 350 ºC for 20 min. The failed (possibly metallic) bonding resulted in Ar gas leakage, rendering the Ar lamp useless. As shown in the right of the figure, the built-in window can be easily dissembled due to the weak bond after annealing.

References:

1. Kaufman, J.; Clark, C., Identification of color centers in lithium fluoride. *The Journal of Chemical Physics* **1963,** *38* (6), 1388-1399.
2. Mador, I.; Wallis, R.; Williams, M.; Herman, R., Production and bleaching of color centers in x-rayed Alkali halide crystals. *Physical Review* **1954,** *96* (3), 617.
3. Laufer, A. H.; McNesby, J., Photolysis of Ethane at the Argon Resonance Lines 1067 and 1048 Å. *The Journal of Chemical Physics* **1965,** *42* (9), 3329-3330.